Wetting Behavior of Human Hair Fibers

Y. K. KAMATH, C. J. DANSIZER, and H.-D. WEIGMANN, *Textile Research Institute, Princeton, New Jersey 08540*

Synopsis

The wetting behavior of human hair in water has been investigated using a technique based on the Wilhelmy balance principle. The experimental technique makes it possible to study the relaxation effects occurring at the solid–liquid–air interface. The results strongly suggest that interactions between the solid and the liquid make important contributions to wettability of the solid surface because of reversible reorientation of polar groups at the interface. The effects of scale structure, weathering, and mechanical damage on wettability of the fiber surface are discussed. Surface roughness of the fiber plays an important role in wetting hysteresis.

INTRODUCTION

Unlike man-made fibers, animal hair fibers are cellular in origin. They consist of a cortex made up of spindle-shaped cortical cells which are enclosed and held together by overlapping flattened cuticle cells. The overlapping arrangement of the cuticle cells imparts a characteristic scaliness to the fiber surface. Compared to other animal hair fibers, human hair has a high degree of overlap of its cuticle cells. At any point the cuticular layer that holds the cortex together may be five to ten cells thick. The individual cuticle cells are enclosed in the epicuticle, a thin layer which appears to be derived from the plasma membrane complex of the outer layer of the developing cuticle cells.[1] The thickness of the epicuticle has been found to be in the range of 2–4 nm. Although no definitive information is available about the epicuticle of the human hair fiber, King and Bradbury[2] have succeeded in isolating the epicuticle of Merino wool and found the analysis to be 78% protein, 5% lipid, and 4% ash. The values may be of a similar order for hair fibers.

From the surface chemical viewpoint, the cortex cells of the human hair fiber are hydrophilic, while the cuticle is hydrophobic, possibly because of the lipid content of the epicuticle. The hydrophobicity of the hair surface is made even more pronounced by the presence of sebum, a waxlike secretion from the sebaceous gland situated at the hair root. However, the hydrophobicity of the hair fiber surface can be strongly affected by environmental oxidative degradation in the presence of sunlight, which generates hydrophilic groups at the surface. Also, mechanical damage of the epicuticle or even of the cuticle as a whole can expose hydrophilic cortical regions. The wetting behavior of a human hair fiber can therefore be used as a measure of the extent of weathering and of mechanical damage suffered by the fiber. Furthermore, the wetting behavior of hair is important to the formulation of modern hair-care products. Many of these products are used in the form of sprays and require that the spray droplets either spread or do not spread on the hair surface before the carrier evaporates. The characterization of the effects of various factors on the wettability of human hair therefore forms the main objective of this work.

0021-8995/78/0022-2295$01.00

THEORETICAL

The equilibrium condition for the forces acting at a solid–liquid–vapor interfaces is given by the Young-Dupré equation

$$\gamma_{LV} \cos \theta = \gamma_{SV} - \gamma_{SL} \tag{1}$$

where γ represents interfacial tension; θ is the contact angle; and the subscripts S, L, and V stand for solid, liquid, and vapor, respectively. The term $\gamma_{LV} \cos \theta$ is defined as the wettability W of the surface.

The interfacial tension between the solid and the liquid, γ_{SL}, is given by

$$\gamma_{SL} = \gamma_{SV} + \gamma_{LV} - A \tag{2}$$

where A is the reversible work of adhesion between the solid and the liquid given by $2\sqrt{\gamma_{SV}\gamma_{LV}}$.[3] Combining eqs. (1) and (2) gives

$$A = \gamma_{LV}(1 + \cos \theta) = \gamma_{LV} + W \tag{3}$$

Since it is a direct measure of the molecular interaction between the solid and the liquid, the work of adhesion is of greater physical significance than the contact angle, which is essentially a geometric parameter. Therefore, all the data are presented in terms of work of adhesion. For the same reason, the wetting hysteresis h is expressed as the ratio of the receding (subscript r) work of adhesion to the advancing (subscript a) work of adhesion:

$$h = \frac{A_r}{A_a} = \frac{1 + \cos \theta_r}{1 + \cos \theta_a} \tag{4}$$

The wetting force of a single fiber measured by the Wilhelmy balance method[4] is given by the equation

$$F_w = w - F_b \tag{5}$$

where w = total wetting force, F_w = electrobalance force reading corrected for the force reading in air, and F_b = buoyancy force on the fiber. The buoyancy force on the fiber is given by

$$F_b = lad \tag{6}$$

where l = immersed length of the fiber, a = area of fiber cross section, and d = density of the liquid. Substituting for F_b in eq. (5),

$$F_w = w - lad \tag{7}$$

Therefore, a plot of F_w as a function of immersion depth l should give a straight line with slope $-ad$ and intercept w. If the perimeter P of the line of contact is known, the wettability W is given by w/P, which according to the Young-Dupré equation is equal to $\gamma_{LV} \cos \theta$:

$$W = \frac{w}{P} = \gamma_{LV} \cos \theta \tag{8}$$

It should be noted that in eq. (7) the sign of the intercept depends on the sign of F_w (i.e., whether the wetting force is positive or negative).

EXPERIMENTAL

Materials

The hair sample used in this work was obtained from DeMeo Bros. of New York and was specified as "European dark brown hair." The sample was cleaned by extracting it with methylene chloride in a Soxhlet extractor and exhaustively rinsing in distilled water. The final washings showed a pH of 6.05. The cleaned hair was dried under vacuum at 50°C and conditioned at 65% R.H. and 70°F. Materials were always protected from dust, and the fibers were handled with tweezers.

The water used for wettability measurements was distilled twice in an all-glass apparatus without using any grease on the joints. Methylene iodide was Fischer purified grade, redistilled under vacuum (38°C/2 mm Hg).

Wetting Force Measurement

The Wilhelmy balance principle has been suggested by a number of investigations[5-7] for the measurement of the wetting force of single fibers and has been used by Bendure[8] to study the dynamic behavior of fibers at oil and water interfaces. The experimental technique adopted here was developed by Miller and Young.[4] The experimental setup used is shown elsewhere[4] and consists of a recording electrobalance (Cahn) and a microscope stage for raising and lowering the liquid level. The microscope stage can be operated manually or at a constant speed using an electric motor, but in this investigation the liquid level was adjusted manually. The fiber is glued to a small wire hook, immersed in water up to a depth of ~10 mm for 30 sec, and then conditioned at 65% R.H. and 70°F. This procedure is used because it has been observed that the wetting force recorded at the first wetting of the fiber is not reproducible, probably due to contaminants on the surface. After counterbalancing the mounted fiber on the beam of the balance, the liquid is raised so that the liquid surface comes into contact with the tip of the fiber. The force is recorded as the fiber is further immersed into the liquid (advancing) and as it is moved out of the liquid (receding).

A typical force recording is shown in Figure 1. The wetting force measured when the fiber first contacts the surface at A may not be a representative value for the surface because the cut end of the fiber may not be flat (this is especially true of hair fibers which have a hydrophilic core and a hydrophobic surface). Therefore, the fiber was immersed in the liquid in steps of 1 mm, and the wetting force was recorded for each step as shown in Figure 1. The fiber is immersed to an immersion depth of 1 mm, and a negative wetting force of the magnitude AB is obtained. When the fiber is stopped the force quickly increases to C. The fiber is again advanced by 1 mm, and the force on the fiber decreases to a level comparable to that at B followed by an increase as before. This variation in force is repeated each time the fiber is advanced by 1 mm. At a total immersion depth of 5 mm, the fiber is left stationary in the liquid, and the wetting force increases significantly from C' to D. Then the fiber is withdrawn from the liquid, giving the receding wetting force E when the tip of the fiber breaks contact with the liquid.

The characteristic time-dependent increase in wetting force at constant immersion depth from C″ to D can clearly be seen in Figure 1. With some fibers
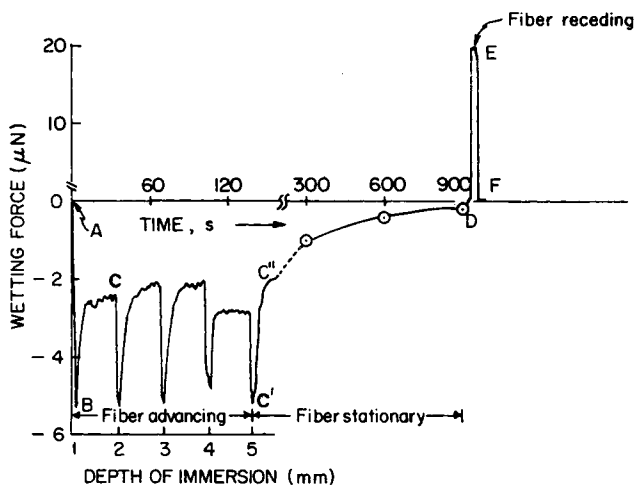
Fig. 1. Wetting force curve (advancing and receding) during stepwise immersion of a human hair fiber into water.

the wetting force levels off, and with others it shows a tendency toward a further slow increase even after extended periods of time. The wetting force D is referred to as the "equilibrium" (subscript e) wetting force, although a state of true equilibrium may not have been reached.

Determination of Fiber Perimeter

Cross sections of human hair fibers of Caucasian origin are generally elliptical in shape. The fiber perimeters were calculated by determining the lengths of the major and the minor axes (the largest dimensions in two perpendicular directions) from microtomed cross sections of the fiber by optical microscopy, using a micrometer eyepiece and assuming a perfectly elliptical cross section. To check the accuracy of this method, the perimeters of fibers reported in Table I were determined from scanning electron micrographs of fiber cross sections and compared with values obtained from measurements of the two axes. The two values agreed within ±3%, thus introducing an error of up to ±3% in the calculated value of wettability. In calculating "equilibrium" and receding wettabilities, a swelling of 10% has been assumed to occur on going from 65% R.H. to

TABLE I
Wettabilities and Related Properties of Human Hair Fibers in Water[a]

Perimeter, μm		211 ± 16
Wetting forces, μN	w_a	−4.55 ± 0.73
	w_e	3.58 ± 0.71
	w_r	15.97 ± 1.53
Wettabilities, mN/m	W_a	−21.0 ± 2.9
	W_e	16.0 ± 2.8
	W_r	67.3 ± 3.3
Work of adhesion, mJ/m^2	A_a	51.8 ± 2.9
	A_e	88.7 ± 2.8
	A_r	140.0 ± 3.4
Wetting hysteresis	h	2.73 ± 0.16

[a] Values reported are averages for 19 fibers at 95% confidence level.

the wet condition. This transverse swelling is based on the value available for wool[9] and has been assumed to be isotropic.

RESULTS AND DISCUSSION

Transient Phenomena in Wetting of Human Hair

Wettabilities of Human Hair. The wetting forces of hair fibers measured by the technique described are given in Table I. Wetting forces were calculated according to eq. (7) using the force readings F_w obtained from the chart (e.g., Fig. 1) at the appropriate depths of immersion. To obtain an advancing wetting force w_a, the minimum force readings (e.g., B and C' in Fig. 1), recorded when new surfaces are offered to the water, were extrapolated to zero immersion depth. The values of wettability W were calculated according to eq. (8). Advancing wettabilities for all fibers are negative and interfiber variations are considerable. It should be noted that the fiber scale direction during immersion was not taken into account in these measurements and also that the fiber snippets were taken randomly along the length of the fibers. It will be seen later that both these factors affect the wetting behavior. High values of advancing wettability and work of adhesion indicate weathering and mechanical damage suffered by the fiber. The time-dependent increase in wettability at constant immersion depth of the fiber in water, that is, the difference between the advancing wettability and the "equilibrium" wettability, may be due to several contributing factors, including the rate of immersion or interfacial velocity and interactions of the keratin surface with the wetting medium. The relative contributions of these factors are discussed in the following paragraphs.

Effect of Interfacial Velocity. Elliott and Riddiford[10] investigated the effects of interfacial velocity on the contact angle for a silicone-treated glass–water–air system. They found no dependence on velocity below 1 mm/min but an increase in contact angle with increasing velocity up to ~10 mm/min. Above this velocity no further increase in contact angle occurred. No attempt was made to measure or control the velocity during the manual immersion of the fibers used to generate the data reported in Table I; however, a rough estimate is ~10–15 mm/min. In an effort to determine the effects of speed of immersion on the measured wetting force, measurements were made on the same fiber used to obtain Figure 1 with the liquid level raised at a speed of ~2.8 μm/sec (0.17 mm/min). The wetting force curve is shown in Figure 2. A comparison of Figures 1 and 2 shows that a higher interfacial velocity does indeed reduce the advancing wetting force (increase the contact angle) slightly. Elliott and Riddiford[10] have explained corresponding effects on the basis that the relaxation times of liquid molecules at the surface are much longer than for those in the bulk liquid. At high entry velocities, liquid molecules at the interface do not have enough time to reorient, resulting in a smaller work of adhesion between the entering solid and the liquid. This leads to a high value of γ_{SL}, given by eq. (2), and consequently to a lower value of wettability as given by eq. (1). Part of the change in wetting force observed immediately after immersion in Figure 1 may be attributed to such an effect of high entry velocity. When the fiber is stopped, the wetting force increases quickly (within seconds) along BC or C'C''. However, only a part of this increase can be due to the orientation of the liquid molecules
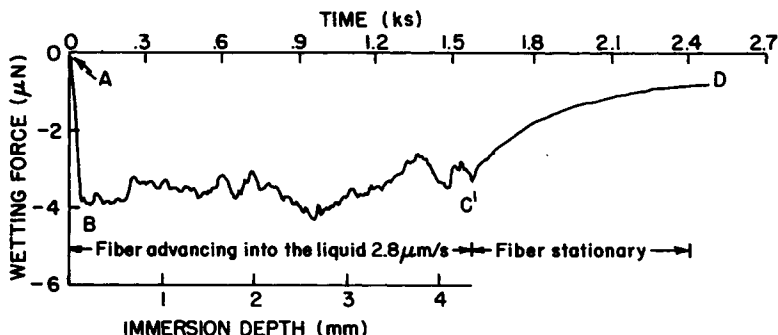
Fig. 2. Wetting forces (advancing) for a human hair fiber (same as in Fig. 1 after drying and re-conditioning) in water at an interfacial velocity of ~2.8 μm/sec (0.17 mm/min).

at the surface, since the slow increase in wetting force when the fiber is stationary (C″ to D in Fig. 1 or C′ to D in Fig. 2) cannot be attributed to the effects of interfacial velocity and must be explained by fiber–liquid interactions.

Wetting Behavior of Nylon and Polypropylene Fibers. In an effort to investigate the role of fiber–liquid interactions in the time-dependent increase in wettability, measurements were made on two fiber types, one interacting strongly with water, the other negligibly (i.e., nylon 6 and polypropylene). Typical wetting force curves for these two fibers are shown in Figure 3. Wettability was determined for fibers conditioned at 65% R.H. as well as for those stored over Drierite in a desiccator. The advancing and "equilibrium" wettabilities with the corresponding works of adhesion are given in Table II.

The results in Table II show that for nylon fibers, either conditioned at 65% R.H. or "dried," values of W_e are significantly higher than those of W_a, whereas for polypropylene, W_e and W_a values are not significantly different. Furthermore, the advancing wettabilities of nylon fibers conditioned at 65% R.H. are significantly higher than those dried over Drierite. Experiments with polypropylene showed no significant effect of conditioning. Figure 3 clearly shows the difference in the time-dependent wetting behavior of nylon and polypropylene. The absence of time-dependent phenomena in the measurement of wetting forces on polypropylene fibers clearly indicates that such phenomena in other fibers must be attributed to interactions of water with the fiber substrate. It is suggested that during penetration of the polyamide, water causes hydrogen bond breakdown in the polymer, thereby increasing molecular mobility in the surface layers and permitting orientation of the polar moieties of the macromolecule toward the liquid surface. Such effects are of course not possible with polypropylene.

Effect of Hair–Liquid Interaction. Wetting measurements were made on hair fibers in both scale directions (against scale, AS, and with scale, WS) in an interacting, swelling liquid (water) and in a nonpolar, nonswelling liquid (methylene iodide). The contact angles were calculated for advancing (θ_a) and "equilibrium" (θ_e) conditions. The difference between these contact angles ($\theta_a - \theta_e$) for each liquid, a measure of the combined effect of the interfacial velocity and the degree of interaction, is given in Table III. The large difference between the $\theta_a - \theta_e$ values for the corresponding scale directions in the two liquids gives support to the hypothesis that solid–liquid interaction is mainly responsible for the time-dependent increase in wettability. The effect of interfacial velocity
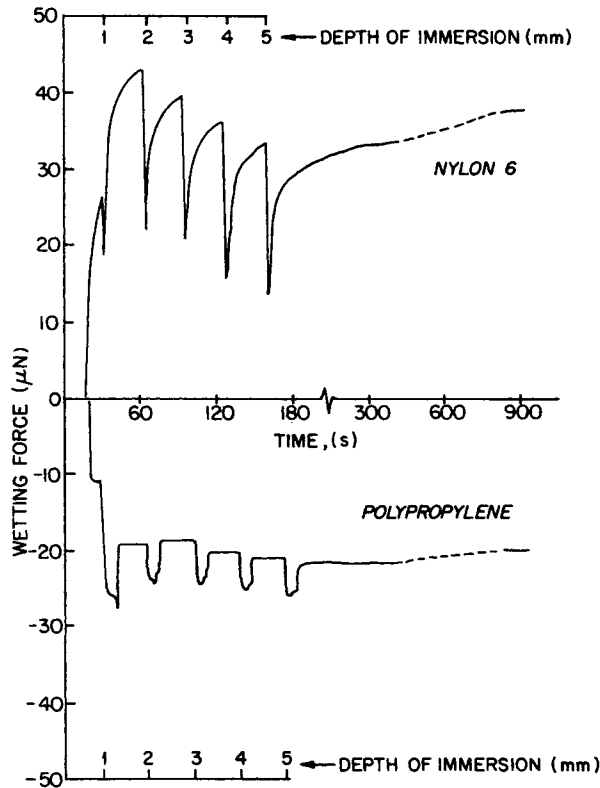
Fig. 3. Wetting force curves during stepwise immersion of nylon 6 and polypropylene fibers in water.

TABLE II
Wettabilities and Works of Adhesion for Nylon and Polypropylene Fibers

Fiber no.	w_a, μN	w_e, μN	P, mm	W_a, mN/m	A_a, mJ/m^2	W_e, mN/m	A_e, mJ/m^2	h
Nylon 6 Conditioned at 65% R.H.								
1	30.6	45.3	1.45	21.0	93.8	31.2	104.0	1.5
2	30.3	37.8	1.47	20.7	93.5	25.8	98.6	1.4
3	30.0	37.8	1.47	20.4	93.2	25.8	98.6	1.4
Nylon 6 Dried								
1	24.1	41.9	1.51	16.0	88.8	27.7	100.5	1.5
2	15.2	35.4	1.50	10.1	82.9	23.5	96.3	1.6
3	19.4	34.4	1.49	13.0	85.8	23.0	95.8	1.5
Polypropylene Conditioned at 65% R.H.								
1	−9.2	−19.2	0.97	−21.2	51.6	−19.8	53.0	—
2	−16.7	−16.3	0.98	−17.0	55.8	−16.6	46.2	1.3
3	−21.0	−21.4	1.02	−20.7	52.1	−21.1	51.8	1.4

is relatively minor. The values of the dispersion and polar contributions to the surface free energy of hair keratin determined by the authors[11] provides further quantitative evidence in support of the above hypothesis.

Reversible Nature of Hair Fiber Wettability. It has been shown above that the advancing wetting force of hair fibers increases with time of immersion.

TABLE III

Difference Between Advancing and "Equilibrium" Contact Angles for Hair Fibers Against Water and Methylene Iodide

Fiber no.	$\theta_a - \theta_e$, deg			
	Water		Methylene iodide[a]	
	AS	WS	AS	WS
1	59	41	−4	−11
2	79	58	10	0
3	78	48	4	14
4	70	54	−7	5
5	84	52	1	4
6	73	60	1	−2
7	75	57	−4	0
8	70	47	9	5
9	74	46	6	6
10	65	55	3	−4

[a] Negative values may not be significant. The interfiber average would, however, be positive and small compared to similar values for water.

In an effort to establish the degree of reversibility of this phenomenon, the wetting force on a fiber was measured during stepwise immersion using 1-mm steps up to a total depth of 5 mm. The fiber was kept in this position until the wetting force reached an "equilibrium" level. Then the fiber was withdrawn and quickly reimmersed in the same way beginning a second cycle. It is unlikely that the fiber dries within this short period of time. Each fiber was taken through four such cycles. The initial advancing wetting forces and the "equilibirum" wetting forces are reported for five fibers in four consecutive cycles in Table IV.

Invariably, the negativity of the initial wetting force was reproducible during four cycles of immediate reimmersion, even though the final or equilibrium wetting force for each cycle in most cases reached positive values. Thus, the initial hydrophobicity of the fiber surface is recovered when the fiber is out of contact with the liquid. It should be noted, however, that there is a small effect of interfacial velocity in these measurements. If the major increase in the wetting force as a function of immersion time is indeed due to molecular orientations at the interface as proposed above, then the reversible nature of this phenomenon may mean that these molecular changes involve rotation of functional groups in the surface regions as a result of breaking hydrogen bonds between protein chains. It seems unlikely that these changes are a result of "macrobrownian"

TABLE IV

Advancing Wetting Forces of Hair Fibers in Successive Immersions (Immediate Reimmersion)

Fiber no.	Initial wetting force, μN				Equil. wetting force, μN			
	1[a]	2	3	4	1	2	3	4
1	−3.76	−3.96	−2.11	−2.46	0.88	−0.53	−0.16	1.92
2	−3.12	−4.22	−2.37	−2.21	1.92	1.74	0.88	−2.08
3	−3.62	−3.06	−3.37	−2.12	3.76	2.41	1.65	2.35
4	−2.97	−2.23	−2.53	−2.48	2.86	1.43	0.90	1.88
5	−3.88	−4.23	−4.34	−4.02	1.96	0.57	1.16	0.31

[a] Wetting cycle.

movements of large segments of the protein molecules. It must be assumed that upon removal of the fiber from the water an unstable water film is formed on the surface of the epicuticle which breaks up into discrete droplets. The surface is now exposed to air allowing reorientation of the hydrophilic groups toward the inside of the fiber and thereby restoring the hydrophobicity of the surface. Similar phenomena have been observed by El-Shimi and Goddard[12] in investigations of the wettability of hoof keratin.

Influence of Surface Topography and Surface Modification on Wetting of Human Hair

Effect of Surface Roughness and Scale Structure. The actual recorder traces obtained during wetting force measurements in water on a human hair and a nylon 6 fiber at a fiber advancing velocity of 2.8 μm/sec (0.17 mm/min) are shown in Figure 4. The nylon fiber is relatively smooth compared to hair with its scale structure, and this is clearly reflected in the nature of the wetting force curves. If sufficient care is taken during the measurements, these curves can be reproduced in repeated runs. This suggests that the small changes in the wetting force are not random but are possibly related to the contour of the fiber. If this is the case, the method would be useful for describing qualitatively the roughness of the fiber surface.

The effect of scale direction was investigated by mounting a single hair fiber on hooks as shown in Figure 5 and cutting the fiber along the line OO′ with a sharp razor blade. The wetting forces were determined by immersing the resulting
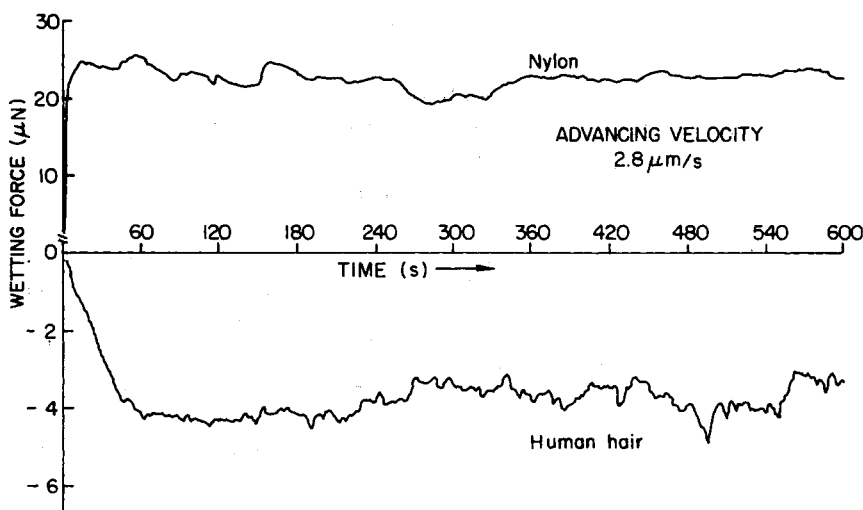
Fig. 4. Wetting force curves for human hair and nylon 6 fibers during immersion into water at an interfacial velocity of ~2.8 μm/sec (0.17 mm/min).
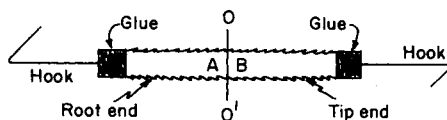
Fig. 5. Schematic representation of the method of mounting human hair fibers on hooks to study the effect of scale direction of immersion on the wetting force.
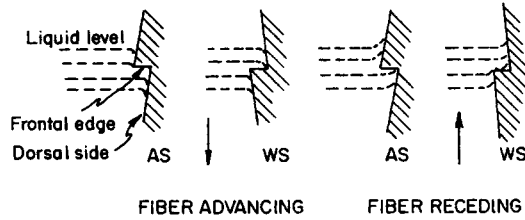
Fig. 6. Effect of scale direction of immersion on the wetting behavior of a human hair fiber in water.

ends A (AS) and B(WS) in the liquid. Wettabilities, works of adhesion, and the hysteresis ratios for several fibers in both scale directions are given in Table V. The data shown in Table V indicate that the advancing wettabilities do not differ very much in the two scale directions but that the receding wettabilities are significantly higher in the AS direction than in the WS direction, causing a higher hysteresis ratio in the AS direction than in the WS direction. For all the fibers examined, $h_{AS} - h_{WS}$ was either zero or positive. It is possible that in the receding mode the liquid surface traverses the contour of the scales better in the AS direction than in the WS direction as illustrated in the schematic drawing in Figure 6 of the liquid traversing a scale edge in the various orientations. It is likely that the frontal edge of the scales has a higher wettability than the dorsal side, since it is more easily affected by mechanical damage, which partially exposes hydrophilic material below the epicuticle. In the receding mode in the AS direction the frontal edges of the scales are wetted because the liquid can contact the contour of the scales more easily. In the WS direction these frontal edges escape proper wetting because the liquid meniscus may be intersecting

TABLE V
Wettability Parameters of Hair Fibers as a Function of Scale Direction[a]

Fiber no.	Scale direction	W_a, mN/m	W_r, mN/m	A_a, mJ/m^2	A_r, mJ/m^2	h	$h_{AS} - h_{WS}$
1	AS	−11.0	55.9	61.8	128.7	2.1	0.2
	WS	−14.5	35.1	58.3	107.9	1.9	
2	AS	−17.1	65.5	55.7	138.3	2.5	0.1
	WS	−24.0	45.4	48.9	118.2	2.4	
3	AS	−20.7	63.3	52.1	136.1	2.6	0.6
	WS	−16.3	41.6	56.5	114.4	2.0	
4	AS	−14.1	62.5	58.7	135.3	2.3	0.3
	WS	−9.7	51.8	63.1	124.6	2.0	
5	AS	−23.4	69.4	49.5	142.2	2.9	0.5
	WS	−25.7	37.8	47.2	110.6	2.4	
6	AS	−14.0	64.2	58.9	137.7	2.3	0
	WS	−17.7	51.9	55.1	124.7	2.3	
7	AS	−13.7	64.9	59.1	137.0	2.3	0.1
	WS	−17.7	50.2	55.2	123.0	2.2	
8	AS	−21.3	58.0	51.5	130.8	2.6	0.5
	WS	−20.4	37.3	52.4	110.1	2.1	
9	AS	−20.8	61.1	52.0	133.9	2.6	0.7
	WS	−13.9	41.1	58.9	113.9	1.9	
10	AS	−10.6	61.1	62.2	133.9	2.2	0.2
	WS	−11.0	52.0	61.8	124.8	2.0	

[a] Letters AS and WS stand for against-scale and with-scale, respectively.

the ridges.[13] In this case the dorsal side of the scales, which is more hydrophobic, makes a greater contribution. This may be the reason for the lower wettability for the WS direction in the receding mode. In general, it should be noted that from the point of view of wetting, a human hair fiber presents a complex surface due to its scale structure and heterogeneity.

Wetting Hysteresis. The causes of wetting hysteresis are not clearly known, and there is no consensus as to how wetting hysteresis should be expressed. Adam[14] merely mentions that the contact angles in the advancing and the receding modes are different but does not give any opinion as to how this could be expressed in a meaningful way. Among the causes of wetting hysteresis, contamination and surface roughness are known to be of considerable importance. Another possible cause of wetting hysteresis could be that the work of adhesion between the solid and the liquid is different for a dry surface as compared to one that has been previously wetted.[14] Therefore, it seems reasonable to express hysteresis as a ratio of the works of adhesion in the receding and the advancing modes, as shown in eq. (4). The magnitude of this ratio would be 1 if there were no hysteresis, and ∞ if the advancing contact angle were 180° and the receding contact angle 0°. The magnitude of the hysteresis can be judged qualitatively from the departure of the ratio from unity.

It is generally observed that the cleaner the surface, the lower is the wetting hysteresis. It appears that adsorbed impurities, even air, interfere with proper wetting of the surface in the advancing mode; but once the surface is wetted, these impurities are desorbed and the liquid wets the surface much better.

Considerable wetting hysteresis has been observed for human hair in this study as shown by the high values (generally greater than 2) shown in Tables I and V. The scale structure seems to be an important contributing factor, since hystersis values for nylon and polypropylene fibers, which are relatively smooth without any scaliness, range from 1.3 to 1.6 (Table II).

Effect of Weathering and Mechanical Damage. As mentioned in the introduction, the degradation of hair keratin under the influence of ultraviolet light from the sun increases the wettability of the surface. It would therefore be reasonable to expect significant differences in wettability between the root and the tip, especially of long hair fibers, which have experienced a long exposure to the atmosphere. Such differences can partly be due also to the absorption of atmospheric pollutants by the hair keratin. According to the work of Valkovic et al.,[15] increasing elemental ratios (element/Zn) have been observed in the hair of subjects as a function of distance from the scalp, where the elements concerned have been identified as the principal pollutants in the area. In an earlier publication, the present authors[11] have found progressively decreasing contact angles from the root end to the tip end of a 0.25-m-long hair fiber.

The natural tips of many long hair fibers have been found to be without any cuticle, and such ends, having the cortex exposed, generally give a positive wetting force. On the other hand, the root section of the same fibers, with cuticle intact, give a negative wetting force.[11] The loss of cuticle toward the tip end seems to be due to chemical degradation of the cuticle combined with mechanical damage caused by handling (such as combing).

Studies in progress deal with the effects on the wetting behavior of hair brought about by controlled surface modification such as abrasion and deposition of polymers.

References

1 R D. B. Fraser, T. P. MacRae, and G. E. Rogers, *Keratins—Their Composition, Structure, and Biosynthesis,* Charles C Thomas, Springfield, Ill., 1972, pp. 70–75.

2. N. L. R. King and J. H. Bradbury, *Aust. J. Biol. Sci.,* **21,** 375 (1968).

3. F. M. Fowkes, *J. Phys. Chem.,* **66,** 382 (1962).

4. B. Miller and R. A. Young, *Text. Res. J.,* **45,** 359 (1975).

5. G. E. Collins, *J. Text. Inst.,* **38,** T73 (1947).

6. R. E. Johnson and R. H. Dettre, *J. Colloid Sci.,* **20,** 173 (1965).

7. F. W. Minor, A. M. Schwartz, E. A. Wulkow, and L. C. Buckles, *Text. Res. J.,* **29,** 940 (1959).

8. R. L. Bendure, *J. Colloid Interface Sci.,* **42,** 137 (1973).

9. P. Alexander, R. F. Hudson, and C. Earland, *Wool—Its Physics and Chemistry,* Franklin Publishing, New Jersey, 1963, p. 87.

10. G. E. P. Elliott and A. C. Riddiford, *J. Colloid Interface Sci.,* **23,** 389 (1967).

11. Y. K. Kamath, C. J. Dansizer, and H.-D. Weigmann, Proceedings of the 9th Congress of the International Federation of the Society of Cosmetic Chemists, Boston, June 1976, p. 523.

12. A. El-Shimi and E. D. Goodard, *J. Colloid Interface Sci.,* **48,** 249 (1974).

13. A. W. Newman, *Adv. Colloid Interface Sci.,* **4,** 105 (1974).

14. N. K. Adam, *The Physics and Chemistry of Surfaces,* Dover, New York, 1968, p. 181.

15. V. Valkovic, D. Rendic, and G. C. Phillips, *Environ. Sci. Technol.,* **9,** 1150 (1975).